Validation of aeroelastic model of Nordtank 500/37

Vølund, P.; Markkilde Petersen, Søren

Publication date:
1997

Document Version
Publisher's PDF, also known as Version of record

RISØ

Risø-R-1006(EN)

Validation of Aeroelastic Model of Nordtank 500/37

Per Vølund and Søren Markkilde Petersen

Risø National Laboratory, Roskilde, Denmark
November 1997

Risø-R-1006(EN)

Validation of Aeroelastic Model of Nordtank 500/37

Per Vølund and Søren Markkilde Petersen

Risø National Laboratory, Roskilde, Denmark
November 1997

Abstract

An aeroelastic model of the stall controlled wind turbine Nordtank 500/37 is validated by comparison of predictions and measurements. The aeroelastic code used is HawC, which has been developed at Risø, and the turbulence model is the Mann model. The measurements used for validation were carried out in the flat terrain of Risø. The model was developed for investigation of load sensitivity to wind and turbulence parameters for complex terrain in the project COMTERID.

The model is found to be good compared to state of the art aeroelastic wind turbine modelling, but the ability of the model to predict the importance of large yaw misalignment is not tested. One limitation of the model is an underestimation of fatigue loads in stall, but for the investigation of parameter sensitivity of complex terrain induced loads, which is meant to be the primary use of the model, this is not important.

The work reported makes part of the project "Investigation of Design Aspects & Design Options for Wind Turbines Operating in Complex Terrain Environments" (COMTERID), which is co-funded through JOULEIII on contract no. JOR3-CT95-0033.

ISBN 87-550-2349-5
ISSN 0106-2840

Information Service Department, Risø, 1997

DISCLAIMER

Portions of this document may be illegible electronic image products. Images are produced from the best available original document.

Contents

1. Introduction

In this report an aeroelastic model of the stall controlled Nordtank 500/37 is validated. The methodology used was developed within the project MOUNTURB, and is described in (Chaviaropoulos et al, 1996). The turbine is a three bladed, upwind and constant speed machine, and is described in (Petersen, 1994). The intention is to use the model for investigation of relative importance of wind and turbulence parameters for loads on wind turbines in complex terrain. This investigation is similar to the one reported for a pitch controlled turbine, Vestas V27, in (Vølund and Petersen, 1996).

2. Description of the aeroelastic code HawC

In this chapter the aero-elastic code "Horizontal axis wind turbine simulation Code", HawC, is briefly described. HawC is described in detail in (Thirstrup Petersen, 1990). HawC has been used for all the response-simulations reported here.

The model is basically a finite element model developed as a special purpose wind turbine model. The rotating substructures, i. e. nacelle and rotor, makes it special compared to general purpose finite element programs. Usually these do not offer a satisfactory modelling of rotating substructures.

The structural model is based on 2-node prismatic beam elements with 6 degrees of freedom at each node, corresponding to 3 translations and 3 rotations. The interpolation functions are polynomials of 3rd order, representing the solutions to the equilibrium equations for the element. The wind turbine structure is subdivided into 3 substructures: tower, shaft/nacelle and rotor. The shaft/nacelle and the rotor are described as rotating substructures, coupled to each other and to the tower. An example of a typical division of the wind turbine in finite elements is shown in Figure 2-1. A more detailed picture of the division in elements on the blade is shown in Figure 2-2.

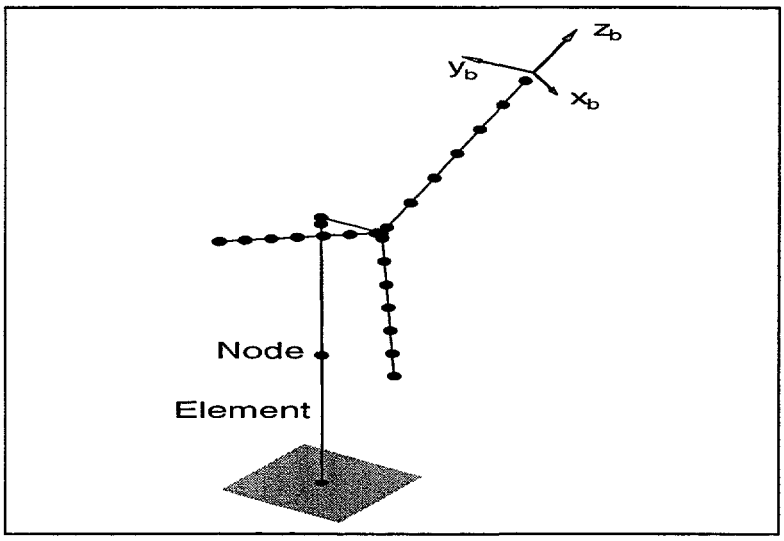

Figure 2-1 Finite element model of wind turbine.

Real blades are tapered and twisted, whereas the available structural finite elements are prismatic, and thus the model is an approximation. In Figure 2-2 a section of the blade is shown in A and the corresponding model in B, where 2 elements are chosen. The (x_b,y_b,z_b)-coordinate system is a common blade system, with the z_b-axis pointing radially outwards. Each element in B is described in a local element coordinate system - for element no. 'i' the system is denoted x_{pi},y_{pi},z_{pi} - with the x_{pi} and y_{pi} axes coinciding with the principal bending axes, and the z_{pi} axis coinciding with the elastic axis. The orientation of the local x_{pi} and y_{pi} axis is usually chosen as the orientation of the principal axes at the midpoint of the real element, resulting in an approximation to the structural blade twist. In the figure the z_{pi} axes are assumed to coincide with the common z_p axis, which need not be the case. In addition to principal bending axes and elastic axis the structural element is described by cross sectional centers for mass and shear.

The aerodynamic geometry is not influenced by the structural element division.

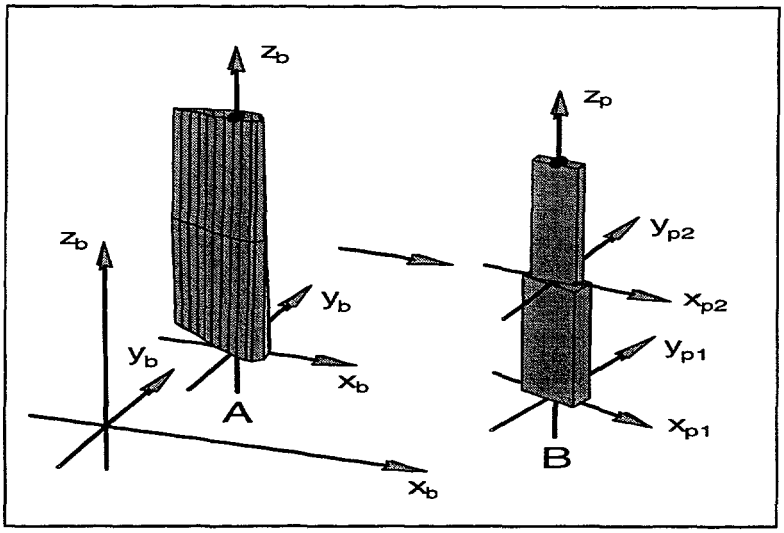

Figure 2-2 Finite elements of blade.

The elastic deformations, including rotations, as well as the bearing restrained rotations at the coupling nodes are taken into account in the expressions for the inertia loads on the substructures. Distributed loads on the elements (inertia, aerodynamic and gravity) are consistently transformed to the nodes. This results in a complete coupled dynamic model for the response of the wind turbine to external loading described by a set of discrete, non-linear, ordinary differential equations with time varying coefficients, comprising the equations of motion, which arranged as a matrix equation has the general form

$$[M]\{\ddot{x}\} + [C]\{\dot{x}\} + [K]\{x\} = \{F\}$$

where

[M] is the mass matrix, which is time varying due to bearing restrained, time dependent changes of geometry,

[C] is the time varying combined structural damping and Coriolis/gyroscopic matrix,

[K] is the time varying combined structural, geometrical and inertia stiffness matrix,

{F} is the force vector composed of terms originating from aerodynamic loads, gravity loads and inertia loads, which have not been resolved in terms which could be included in the left hand side expressions

{x} is the vector of translations and rotations

The flexible elements of the drive train are modelled as shaft elements with mass, structural damping and stiffness. The generator is modelled as a separate rotational degree of freedom with mass moment of inertia and a torque corresponding to the actual generator characteristic, which can be explicitly prescribed in a subroutine. An asynchronous generator is used for the turbine involved in the present work. Its characteristic is equivalent to a damping term, which can be adequately derived from the slip and the nominal torque. All properties of high speed shaft elements and generator are transformed to the low speed shaft side of the gear box.

The model offers the possibility of calculating the coupled mode shapes and natural frequencies for the rotating turbine as well as for the turbine at stand still. The facility is frequently used to compare the dynamic properties of the modelled turbine with the properties of the real one, for which the fundamental frequencies have often been determined with good accuracy. This check is further a guideline for choosing an appropriate number of elements in the finite element model.

The structural damping is modelled as proportional damping, i.e. a linear combination of the mass and the stiffness matrices. Choice of its actual magnitude is based on experience. Its inclusion is important, when considering dynamic activity at, or close to, the natural frequencies.

Aerodynamic load and wind field

The aerodynamic loads are derived by use of a quasi-steady theory, based on combined blade element and momentum theory. The calculation of induced velocity can be based on either the frozen wake or the equilibrium wake approximation.

No model for dynamic inflow has been included in the code so far. All the results presented in the present work have been based on the frozen wake approximation.
The model for aerodynamic load calculation is fully aero-elastic, in that the influence of the elastic deformations on the aerodynamic force is taken into account.

The pitch control in the model is equivalent to the control on the real turbine. The blade is pitched both structurally and aerodynamically, controlled by an algorithm, which can be identical with the one on the real turbine.

The free wind vector is composed of a deterministic contribution including wind shear and tower interference, and a stochastic component, which is generated according to the Mann method for time simulation of turbulence.

Turbulence model

The Mann turbulence simulation method is based on a recently developed model of a spectral tensor for atmospheric surface layer turbulence at high wind speeds, corresponding to neutral stratification. The model is described in (Mann, 1994). The model assumes that the turbulence is homogeneous in space but non-isotropic and includes the influence of shear. The method generates a full three-dimensional turbulence field with all three components.

The turbulence is generated in a rectangular box with quadratic cross section corresponding to the plane perpendicular to the mean wind direction at points placed on a rectangular grid. In the present application of the method there are 16*16 points available on a quadratic grid on a cross section and 4096 points in the along wind direction. The grid points are approximately equally spaced in all directions. The generated turbulence is scaled and stored on disk. The only parameters needed for scaling to actual conditions are hub height, mean wind speed and terrain roughness length.

In order to obtain a reasonable turbulence for complex terrain from the homogeneous Mann field a facility has been added to the aero-elastic code, which offers the possibility of scaling the turbulence intensity individually for the 3 directions. This will of course add some distortion to the spatial structure of the turbulence, which may not be in agreement with the actual measured field.

The wind shear is described by either a log- or a power-law, or alternatively the shear field might be predefined through definition as a vector field on an planar grid perpendicular to the mean wind direction at hub height, which is read from a file.

The tower interference is taken into account by use of a potential flow model. An example of the longitudinal v_y component of an arbitrary predefined shear field influenced by the tower is shown in Figure 2-3.

Solution of equations of motion

The equations of motion are solved at each time step by use of the Newmark implicit time integration scheme. Iterations are performed at each time step in order to obtain equilibrium within certain prescribed limits.

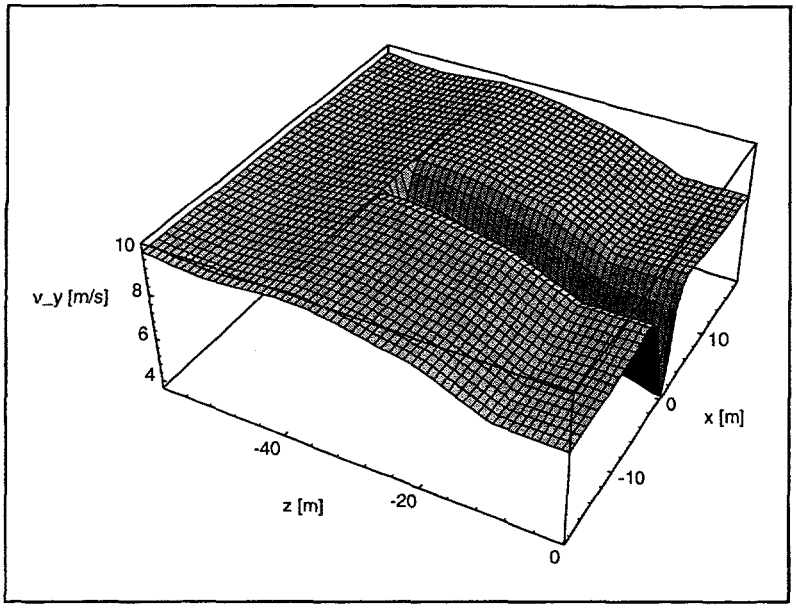

Figure 2-3 Predefined shear (longitudinal component) influenced by tower. z=0m corresponds to ground level.

3. Validation of aeroelastic model

In this chapter predictions are compared with measurements from the flat terrain of Risø.

3.1 3D-correction of lift coefficients

It was decided **not** to modify the 2-dimensional lift coefficients for 3-dimensional effects on the rotor. Input for such corrections are proposed by (Rasmussen et al, 1988) and (Aagaard Madsen, 1991) and others, but no good investigation exists of the 3D-effects in stall. At the same time the importance of such a correction for the parameter-identification, which is the aim of the modelling, is thought to be small.

Figure 3.1-1 show the used 2-dimensional Cl-data. The data within the alpha-range -10 to 110 deg. originate from (Abbot and Doenhoff, 1959), but have been modified by Stig Øye, DTU, Denmark, and the interval has been extended to cover -180 to 180 deg. by Per Vølund, Risø, Denmark.

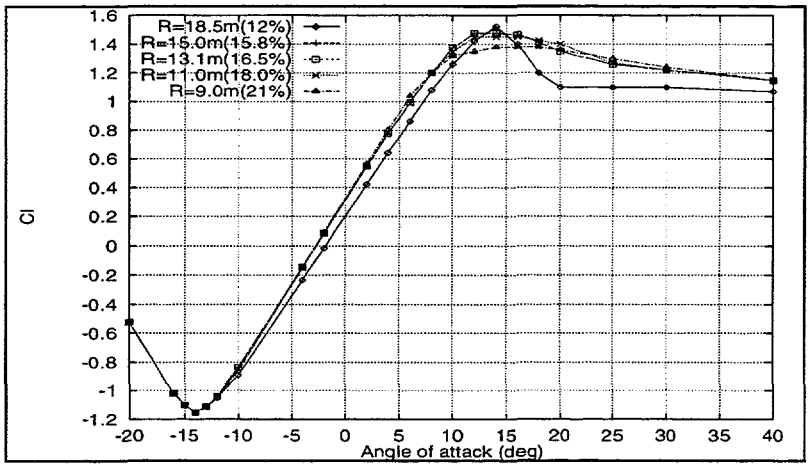

Figure 3.1-1 2-dimensional Cl-data originating from (Abbot and Doenhoff, 1959).

3.2 Statistics of measurements and predictions

For validation of the model selected results are compared with measurements from Risø. In all cases 10-minute series sampled with 32 Hz have been used. The turbulence intensity for measurements are in the range 10-15% and for the simulations 12.5%.

Figure 3.2-1 shows mean-values of measured and predicted flapwise blade bending moments. A difference in mean levels of around 25 kNm is seen. A small part of the difference, 3 kNm, is due to different definitions of the 0 level - for measurements 0 corresponds to 0 aerodynamic forces, for predictions 0 corresponds to 0 aerodynamic forces and 0 gravity forces (consequently tilt causes a difference).

Figure 3.2-2 shows the maximum, minimum and mean values of the measured and predicted flapmoments. All measued values have been corrected by the 25 kNm difference found in Figure 3.2-1. Apparently the model underestimates the extremes of the flapmoment at high and low wind speeds.

Figure 3.2-3 shows the standard deviation of measured and predicted flapmoments. Apparently the model underestimates the standard deviation of the flapmoment at high and low wind speeds. At high wind speeds the underestimation is around 35%, and for normal operation predicted life-time equivalent flapmoment can thus be expected to be underestimated by as much as 35%.

Figure 3.2-4 shows for the wind speed the mean, maximum and minimum of the measured and predicted time series. Predictions slightly underestimates the maximum to minimum range - even though the average standard turbulence intensity for the measurements is equal to the 12.5% used for the predictions.

Figure 3.2-5 shows for the edgewise moments mean, maximum and minimum of the measured and predicted time series. The strain gauges are mounted on the hub and the measured edgemoment is known to be strongly influenced by changes of the strain-pattern at increasing wind speed and flapload. For this reason the differences between measured and predicted edgemoment doesn't tell much.

Figure 3.2-6 shows shaft torsion measured and predicted mean, maximum and minimum values. The 0-value is seen to drift a lot.

Figure 3.2-7 shows electrical power measured and predicted mean, maximum and minimum values. The maximum to minimum level is seen to be underestimated in the predictions - exactly as the flapmoment-range is underestimated as commented for Figure 3.2-3 above.

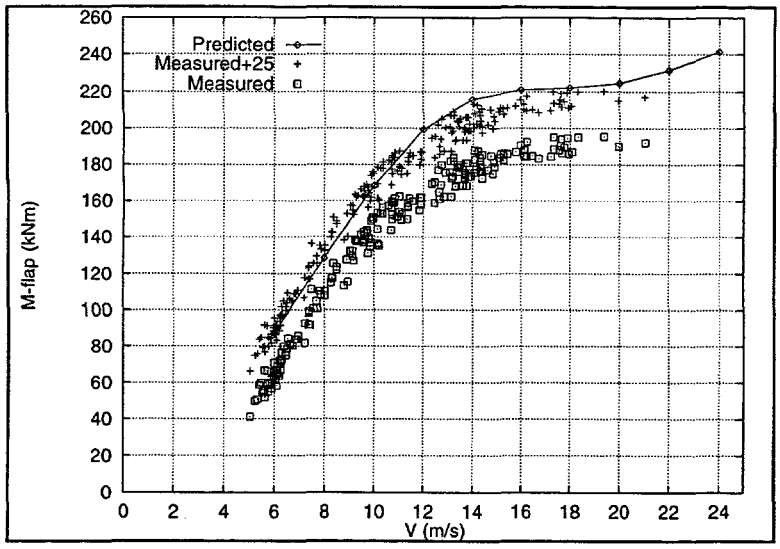

Figure 3.2-1 Mean of measured and predicted flapwise moments.

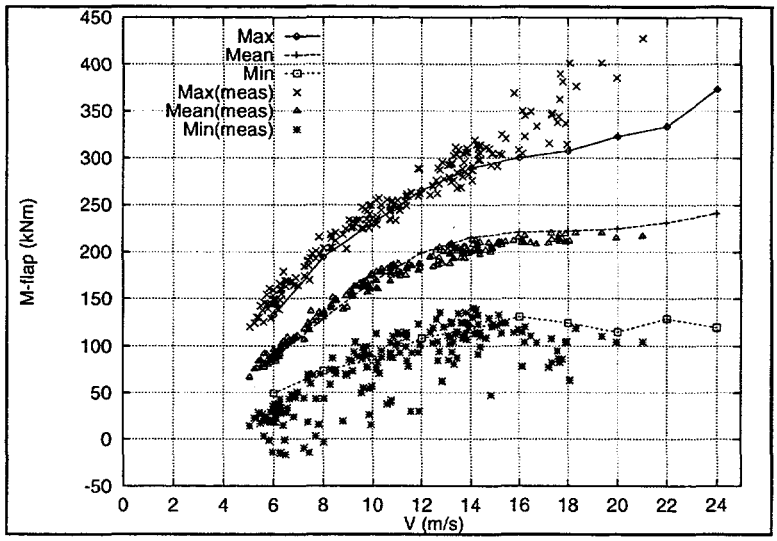

Figure 3.2-2 Mean, maxi. and min. of measured and predicted flapwise moments.

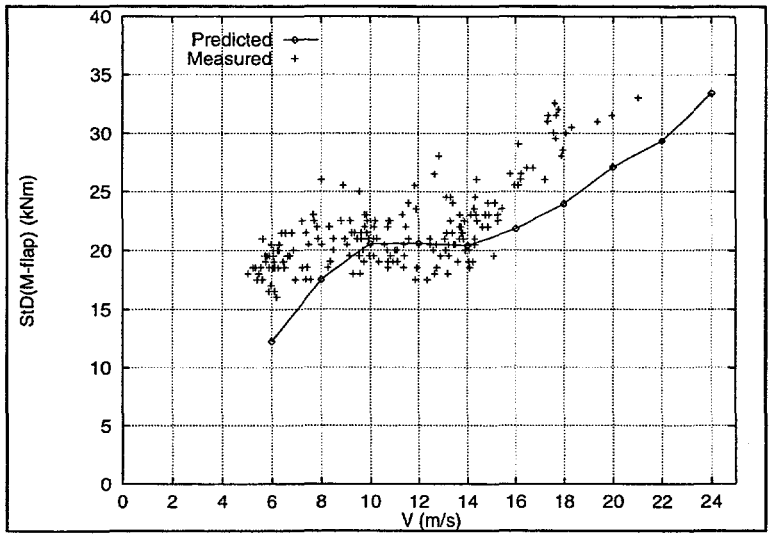

Figure 3.2-3 Standard deviations of measured and predicted flap bending moments.

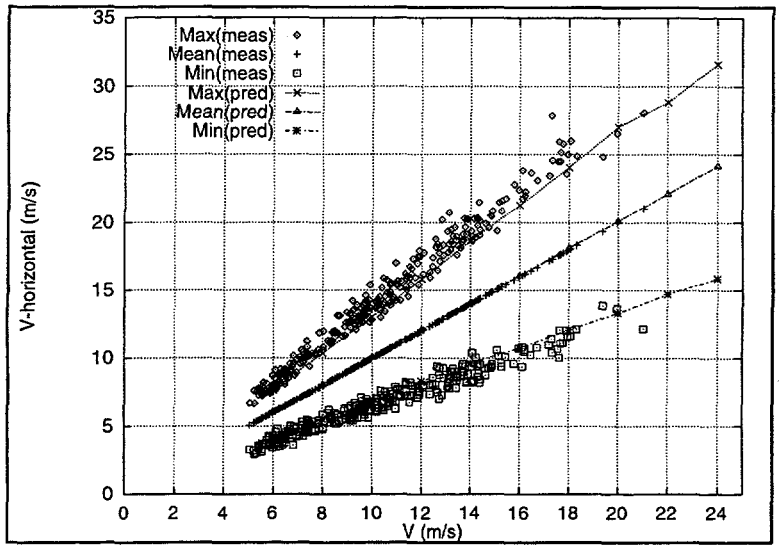

Figure 3.2-4 Mean, max. and min of measured and predicted horizontal wind speed.

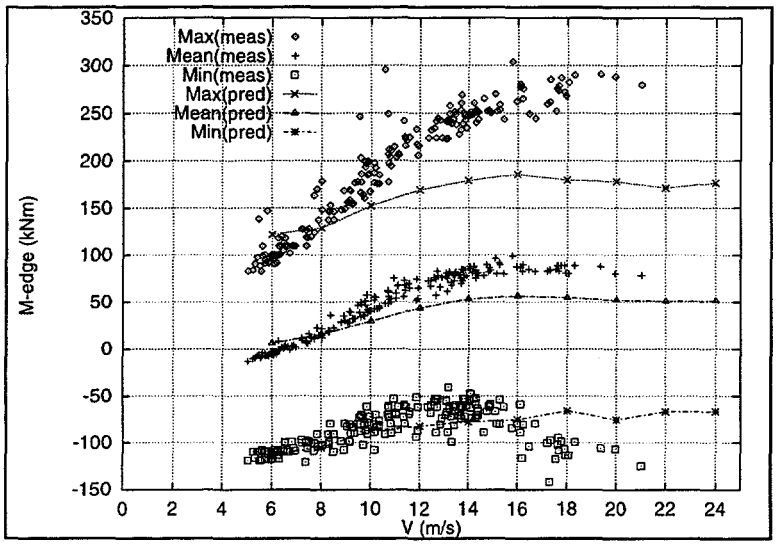

Figure 3.2-5 Mean, max. and min. of measured and predicted edgewise moments.

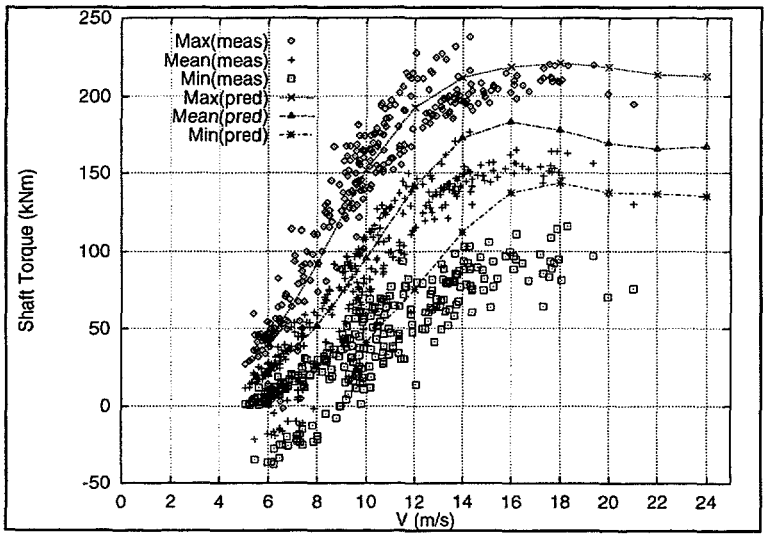

Figure 3.2-6 Mean, max. and min. of measured and predicted shaft torsion.

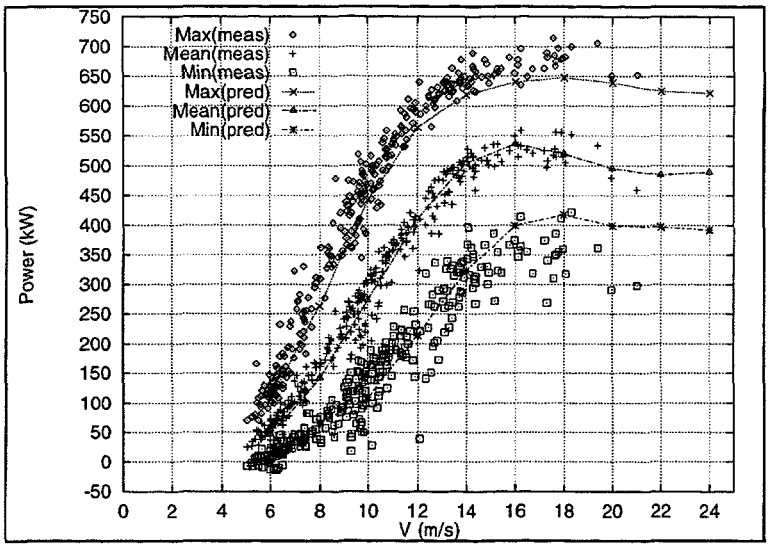

Figure 3.2-7 Mean, max. and min. of measured and predicted electrical power.

3.3 Power spectra of measurements and predictions

The power spectra presented here correspond to 10-minute time series sampled at 32 hz. The power spectra have been averaged over 16 parts. Mean wind speed, yaw-error and turbulence intensity for the three time series used for validation is shown in Table 3.3-1.

	10 m/s	14 m/s	18 m/s
Mean (V) (m/s)	10.42	13.97	17.96
Mean (Yaw) (deg)	-11.0	5.0	6.0
Turbulence Intensity (%)	17.7	11.7	11.8

Table 3.3-1 *Selected data for the 3 time series used for evaluation of the model.*

Figure 3.3-1, Figure 3.3-2 and Figure 3.3-3 show power spectra of horizontal wind speed measured and predicted at 10, 14 and 18 m/s respectively. The differences at low frequencies are partly due to the chosen averaging over 16 short pieces of the time series. The predictions are carried out with the Mann model. The measurements are carried out with a cup anemometer and due to its cut-off frequency the energy content at frequencies above 0.8 Hz is underestimated. Predictions are seen to underestimate the energy content above 0.8 Hz even more than the cup anemometer measurements - the reason is probably not the u-direction-resolution of the turbulence as the cut-off frequency is seen not to change from 10 to 14 and 18 m/s, whereas it could be due to the quadratic 16*16 resolution over the rotor-disc - or an inherent quality of the Mann model? The cutting off of energy at frequencies higher than 0.8 Hz is anyway believed not to influence the predicted loads significantly.

Figure 3.3-4, Figure 3.3-5 and Figure 3.3-6 show power spectra of measured and simulated flap moments at 10, 14 and 18 m/s respectively. The same data are plotted logarithmically in Figure 3.3-7, Figure 3.3-8 and Figure 3.3-9. 1P is 0.5 Hz, 2P is 1.0 Hz etc. In measurements as well as simulations the dominating energy content is found at 1P, as is usual for homogeneous terrains, but even stronger at 10 m/s due to the yaw-error of 11 degrees. At 18 m/s a difference between measurement and prediction is found at 2 Hz - this difference is strongly sensitive to the choice of parameter for the stall model.

Figure 3.3-10, Figure 3.3-11 and Figure 3.3-12 show power spectra of measured and simulated edge moments at 10, 14 and 18 m/s respectively. The dominating energy content is found at 1P, but also the edgewise blade eigenfrequency of around 3.5 Hz (7P) is

pronounced. The measurement is influenced by the flapwise bending moment, and in the range 1 to 3 Hz this influence dominates the signal, because the energy content of the edgewise bending moment is close to 0, as can also be seen in the predictions. The measured signal should thus be used with reservations only.

Figure 3.3-13, Figure 3.3-14 and Figure 3.3-15 show power spectra of measured and simulated electrical power at 10, 14 and 18 m/s respectively. At 18 m/s a considerable difference is seen at frequencies over 0.4 Hz - the energy content of the prediction is low. This is thought to be due to the stall model - see Appendix A.

Figure 3.3-16, Figure 3.3-17 and Figure 3.3-18 show power spectra of measured and simulated shaft torque at 10, 14 and 18 m/s respectively. The result is very similar to the result for electrical power in Figure 3.3-13, Figure 3.3-14 and Figure 3.3-15.

Figure 3.3-19, Figure 3.3-20 and Figure 3.3-21 PSD of measured and predicted shaft bending moment at 18 m/s. show power spectra of measured and simulated shaft bending moment at 10, 14 and 18 m/s respectively. Some difference is seen at frequencies above 2 Hz, where the energy level is very low. In the range 0.6-2.0 Hz measurements and predictions show very little difference. At 1P the difference between predictions and measurements is significant. The reason for this is that for the predictions the yaw position is constant and the yaw misalignment is identical to the mean yaw misalignment in measurements (see Table 3.3-1), whereas for the measurements the turbine is yawing as shown in Figure 3.3-24, Figure 3.3-25 and Figure 3.3-26. Yaw misalignment either increases or decreases the gravity induced deterministic 1P variation of the shaft bending (and at the same time increases or decreases the mean level of the tilting moment) - and because simulations and predictions on this point is quite different the energy content of the spectra at 1P are also much different.

Figure 3.3-22 and Figure 3.3-23 show measured and predicted power spectra of tilt moment and yaw moment at 18 m/s. Measurements and predictions are seen to have only small differences.

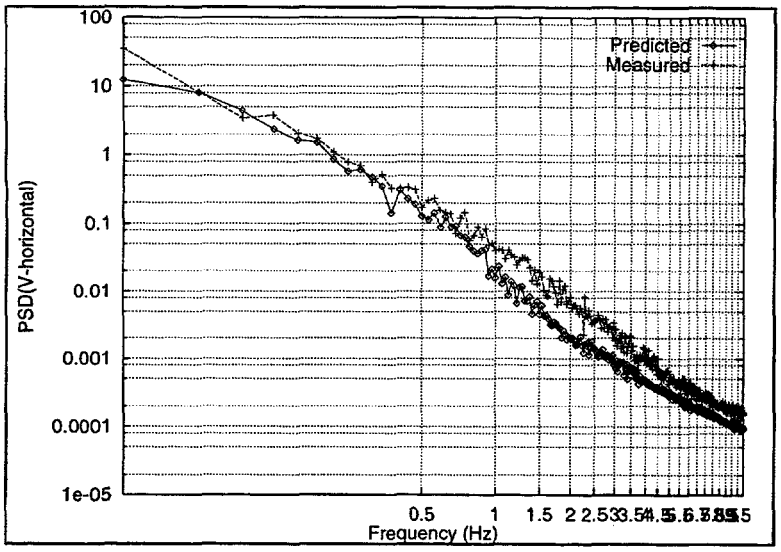

Figure 3.3-1 PSD of measured and predicted wind speed at 10 m/s.

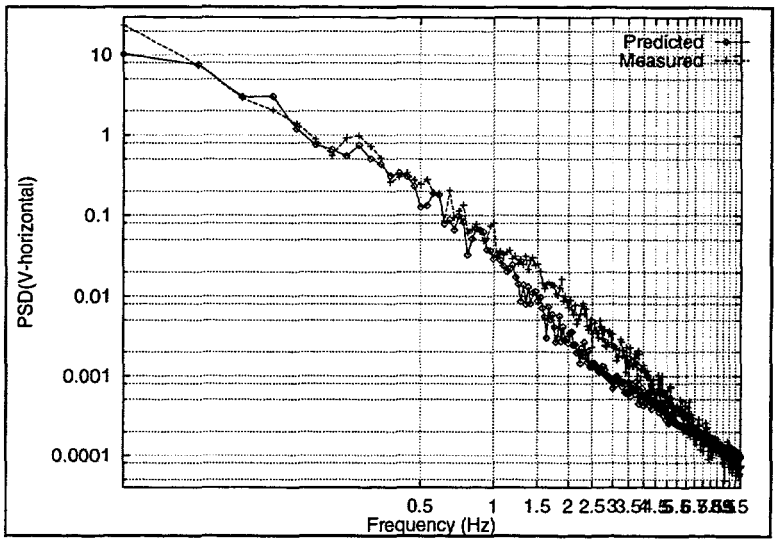

Figure 3.3-2 PSD of measured and predicted wind speed at 14 m/s.

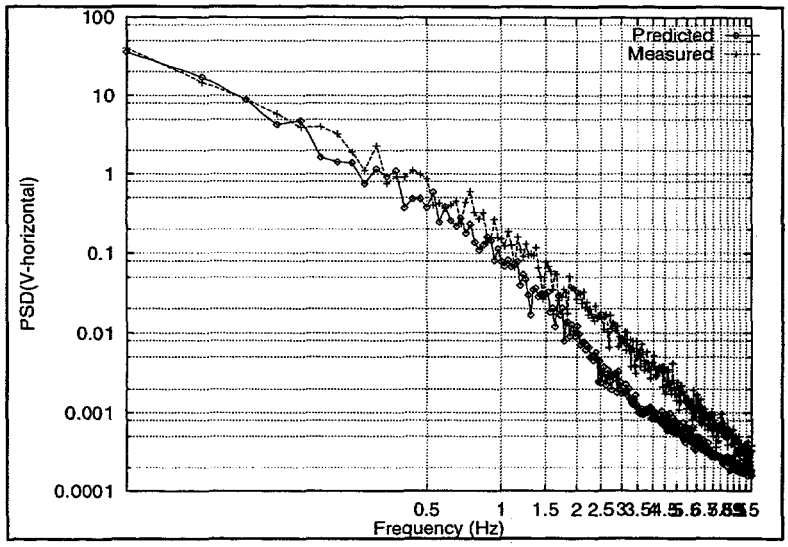

Figure 3.3-3 PSD of measured and predicted wind speed at 18 m/s.

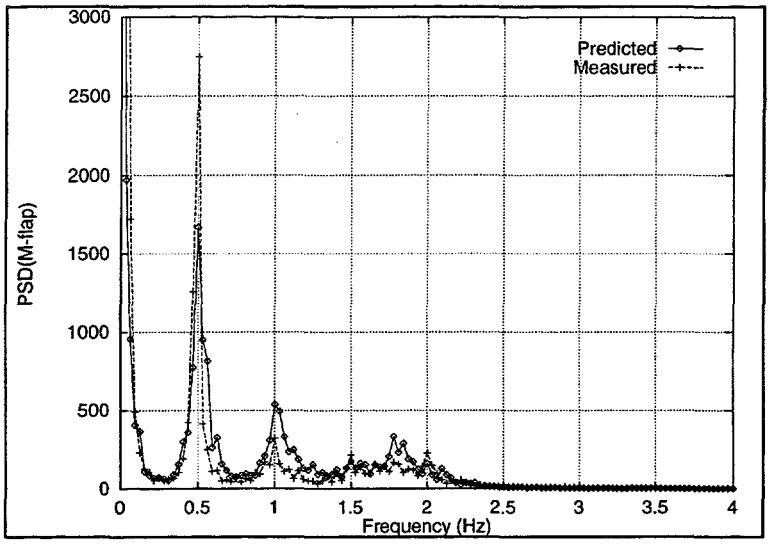

Figure 3.3-4 PSD of measured and predicted flapmoments at 10 m/s.

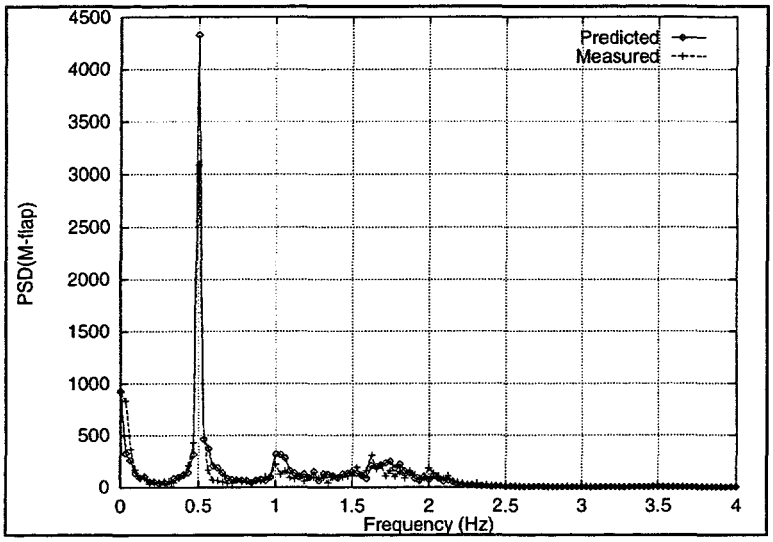

Figure 3.3-5 PSD of measured and predicted flapmoments at 14 m/s.

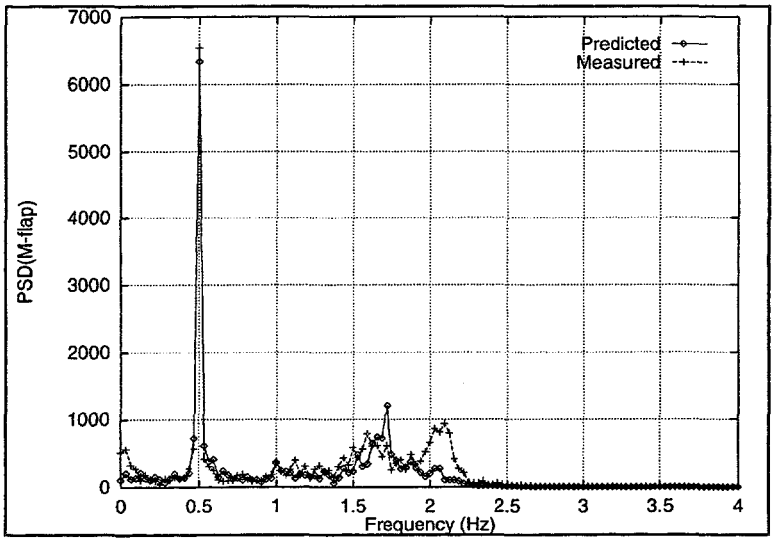

Figure 3.3-6 PSD of measured and predicted flapmoments at 18 m/s.

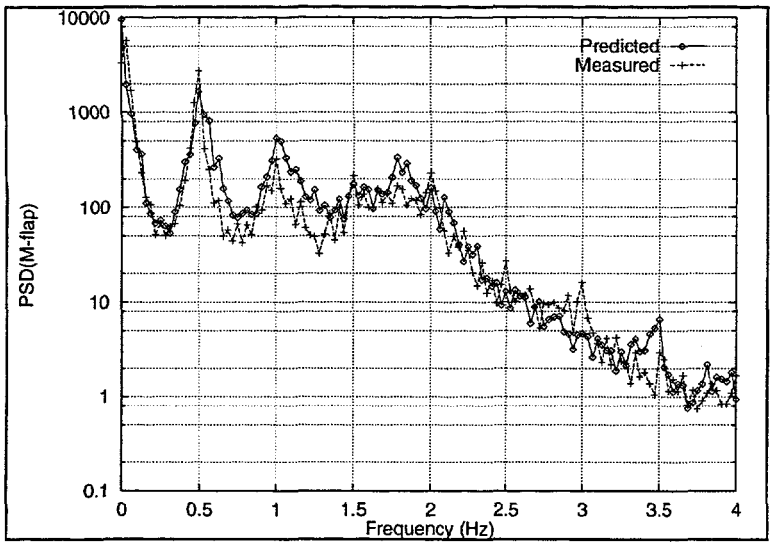

Figure 3.3-7 PSD of measured and predicted flapmoments at 10 m/s.

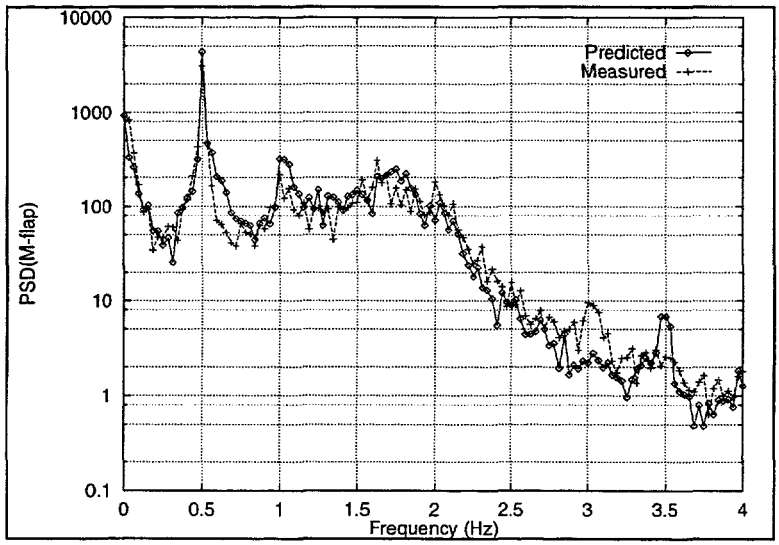

Figure 3.3-8 PSD of measured and predicted flapmoments at 14 m/s.

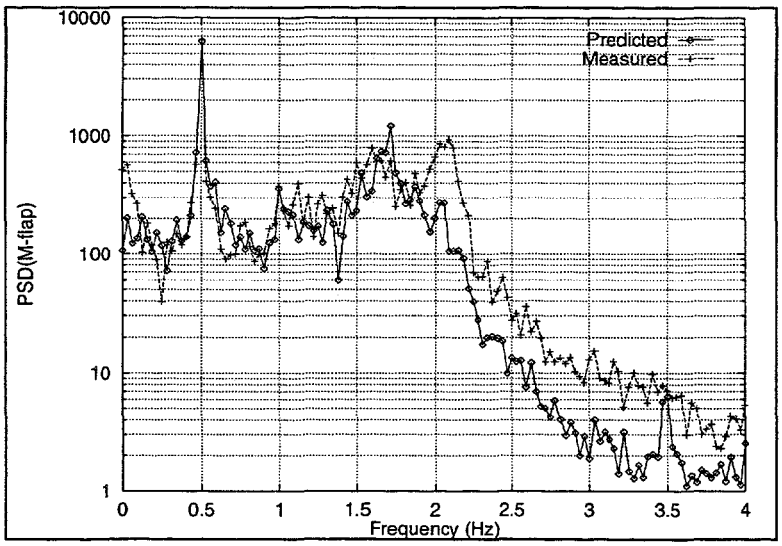

Figure 3.3-9 PSD of measured and predicted flapmoments at 18 m/s.

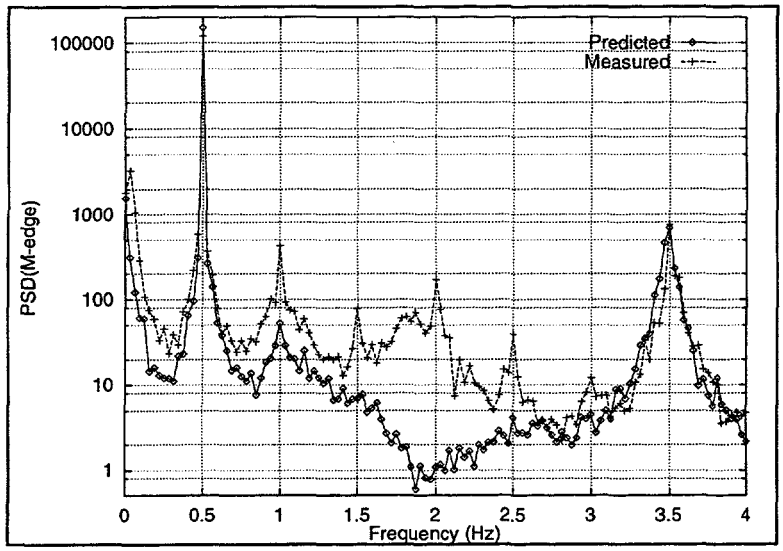

Figure 3.3-10 PSD of measured and predicted edgemoments at 10 m/s.

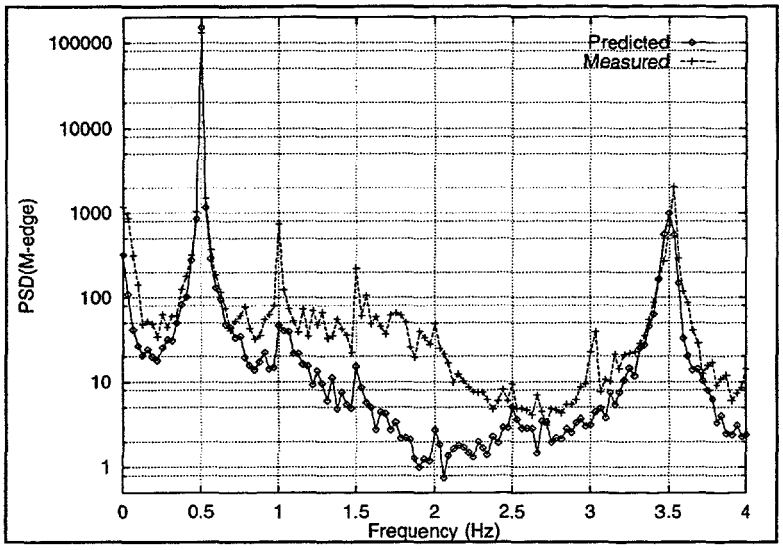

Figure 3.3-11 PSD of measured and predicted edgemoments at 14 m/s.

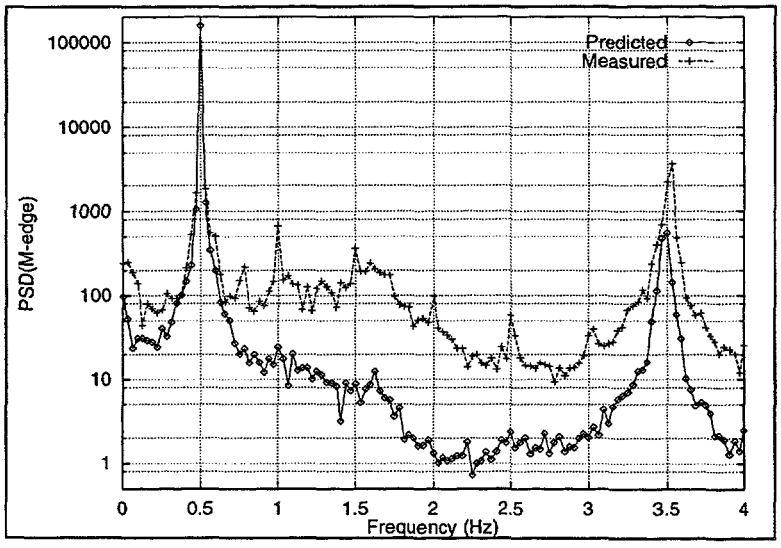

Figure 3.3-12 PSD of measured and predicted edgemoments at 18 m/s.

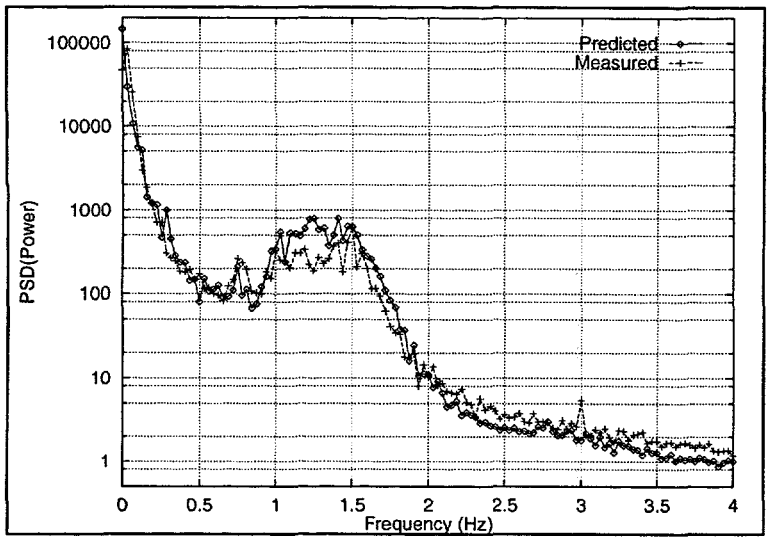

Figure 3.3-13 PSD of measured and predicted power at 10 m/s.

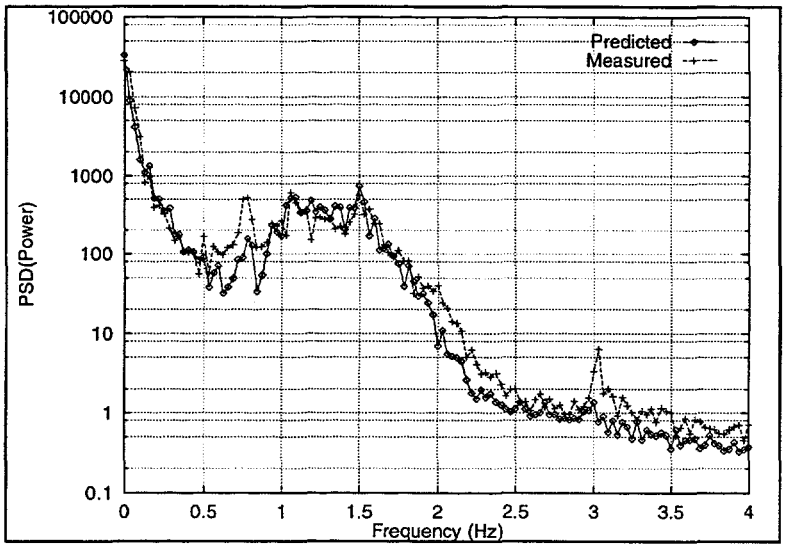

Figure 3.3-14 PSD of measured and predicted power at 14 m/s.

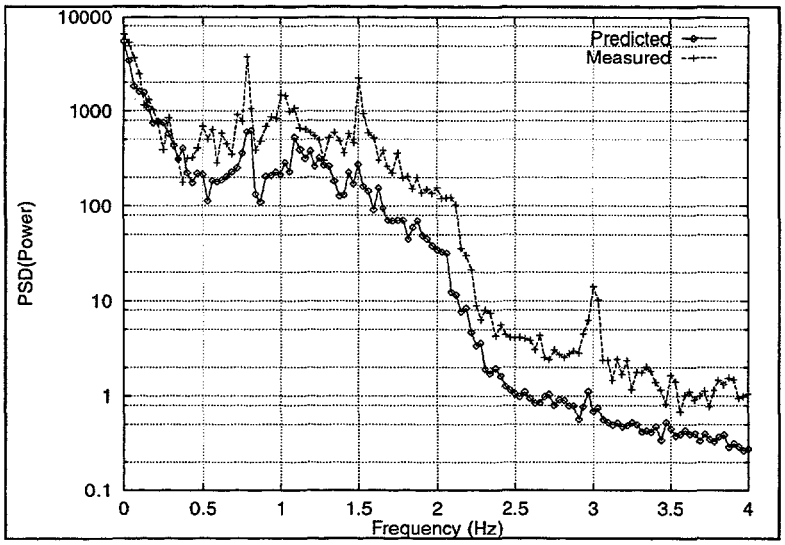

Figure 3.3-15 PSD of measured and predicted power at 18 m/s.

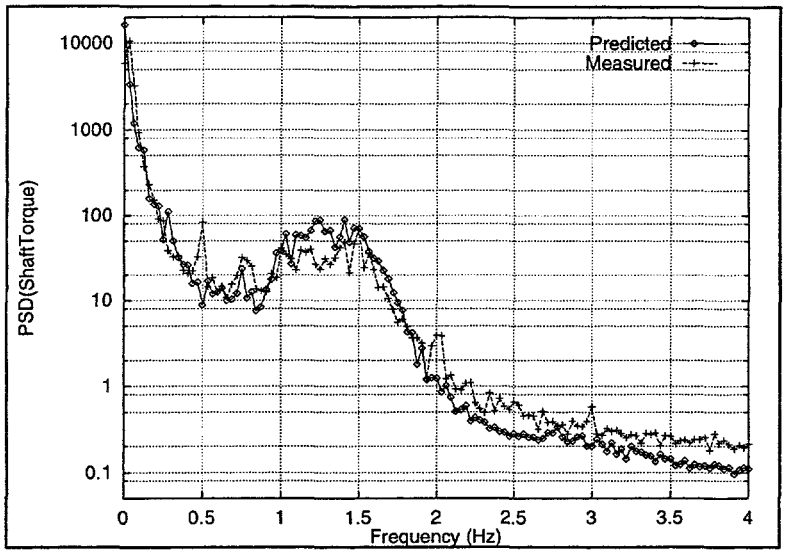

Figure 3.3-16 PSD of measured and predicted shaft torsion at 10 m/s.

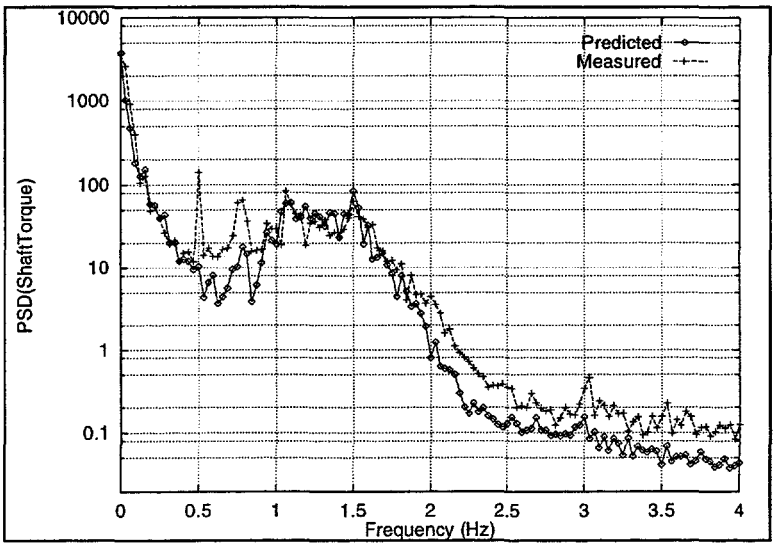

Figure 3.3-17 PSD of measured and predicted shaft torsion at 14 m/s.

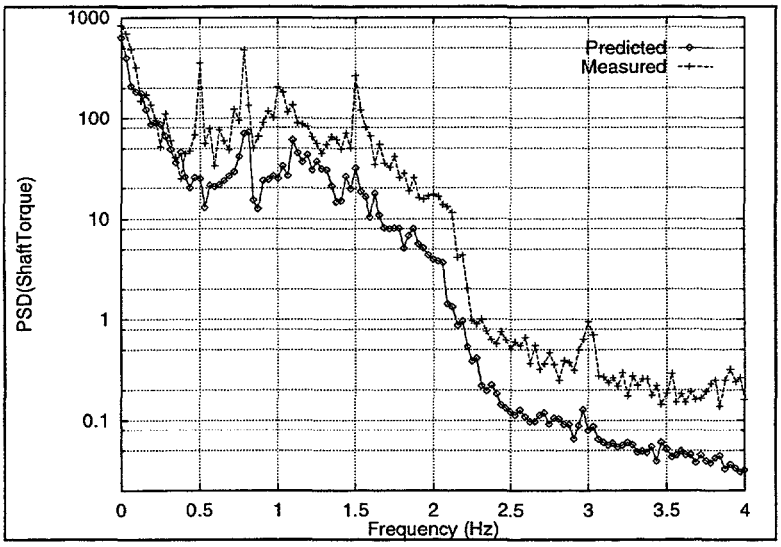

Figure 3.3-18 PSD of measured and predicted shaft torsion at 18 m/s.

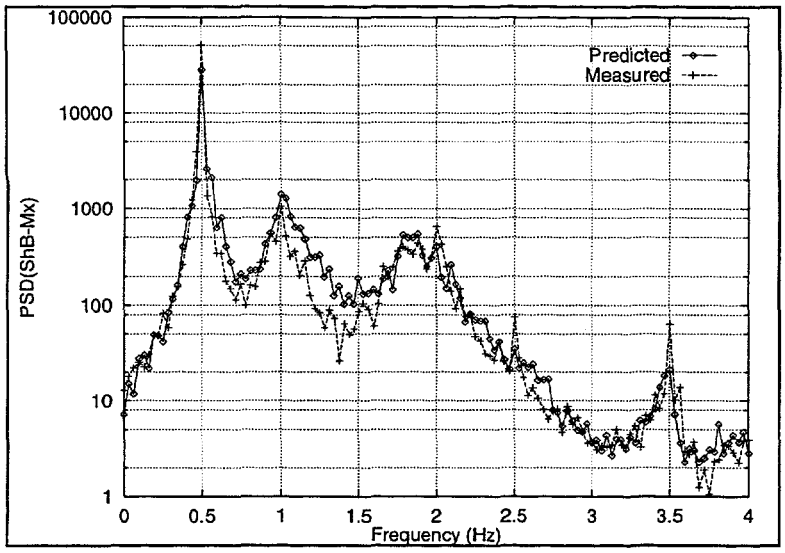

Figure 3.3-19 PSD of measured and predicted shaft bending moment at 10 m/s.

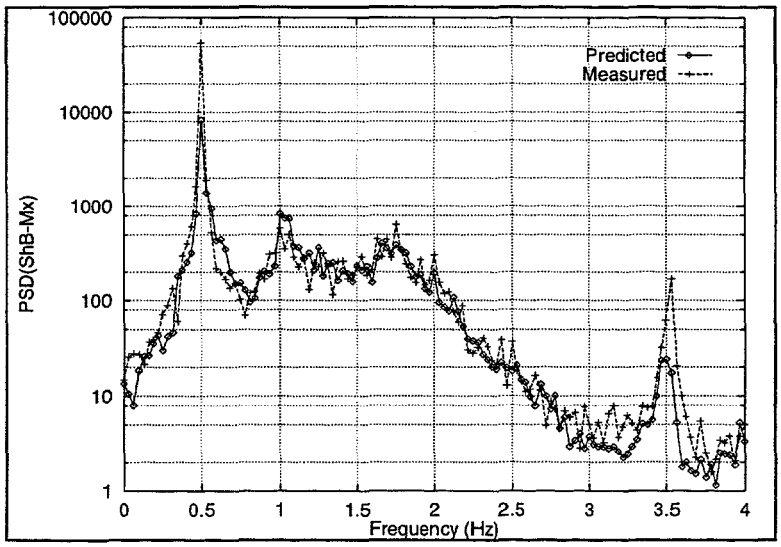

Figure 3.3-20 PSD of measured and predicted shaft bending moment at 14 m/s.

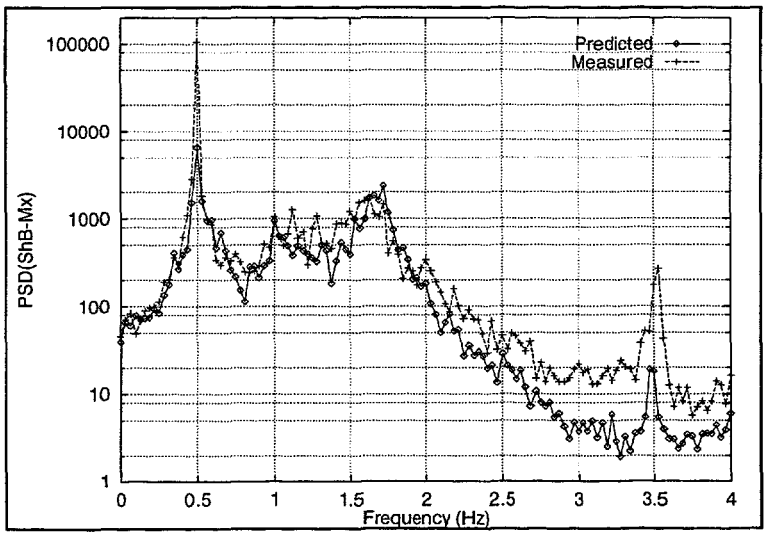

Figure 3.3-21 PSD of measured and predicted shaft bending moment at 18 m/s.

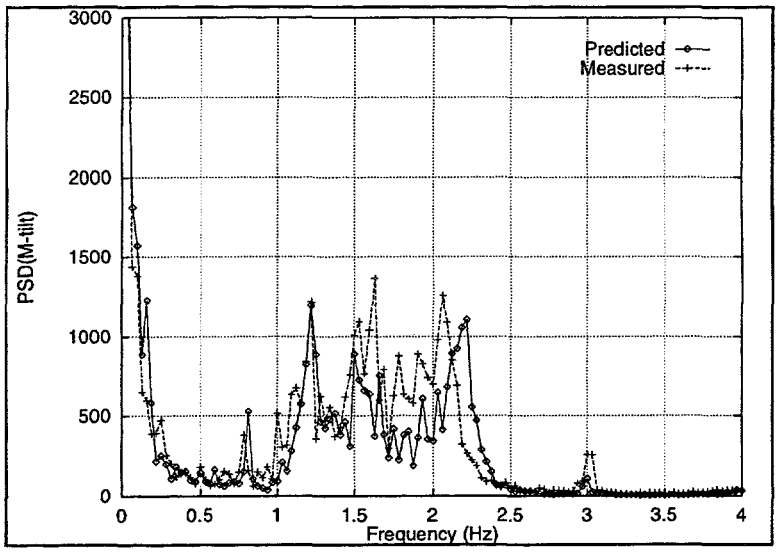

Figure 3.3-22 PSD of measured and predicted tilt moment at 18 m/s.

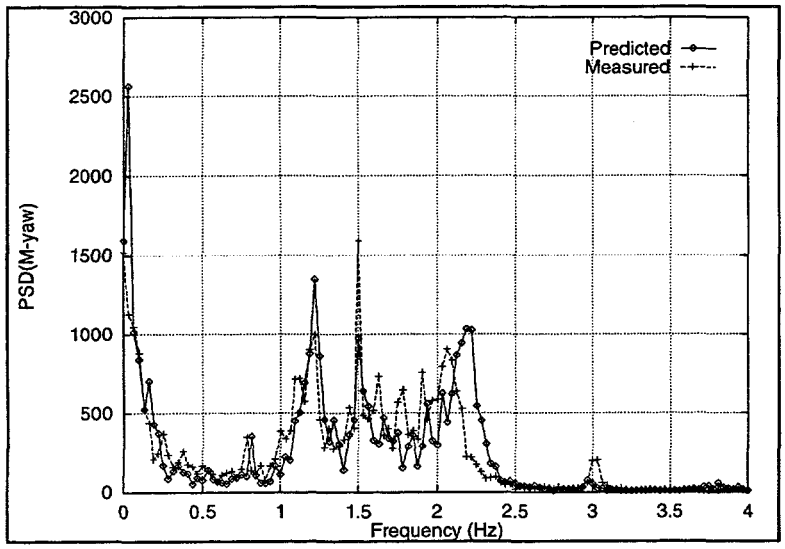

Figure 3.3-23 PSD of measured and predicted yaw moment at 18 m/s.

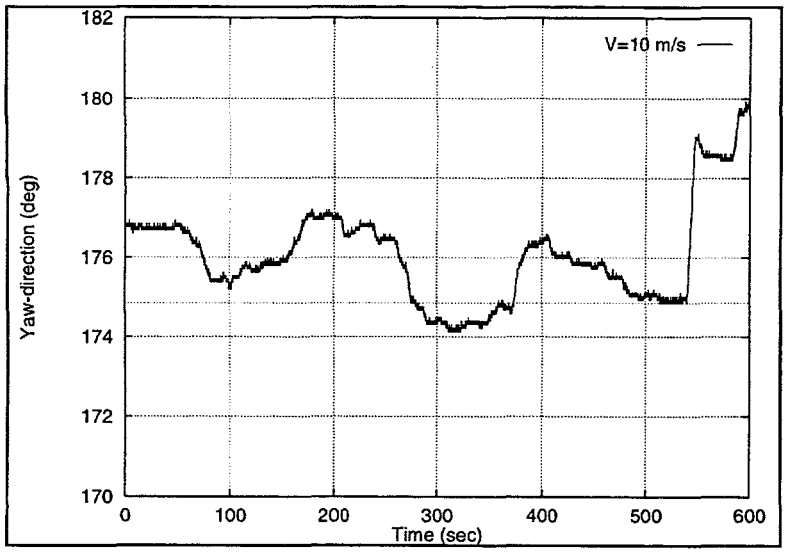

Figure 3.3-24 Time-track of measured yaw direction at 10 m/s.

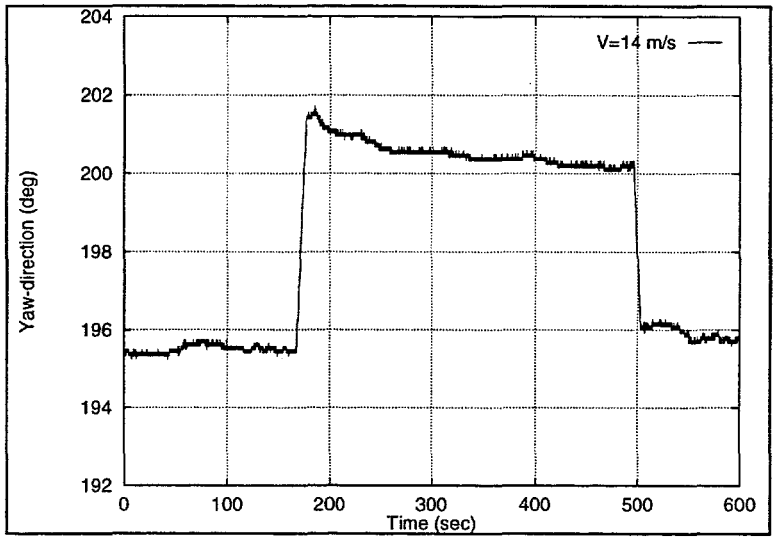

Figure 3.3-25 Time-track of measured yaw direction at 14 m/s.

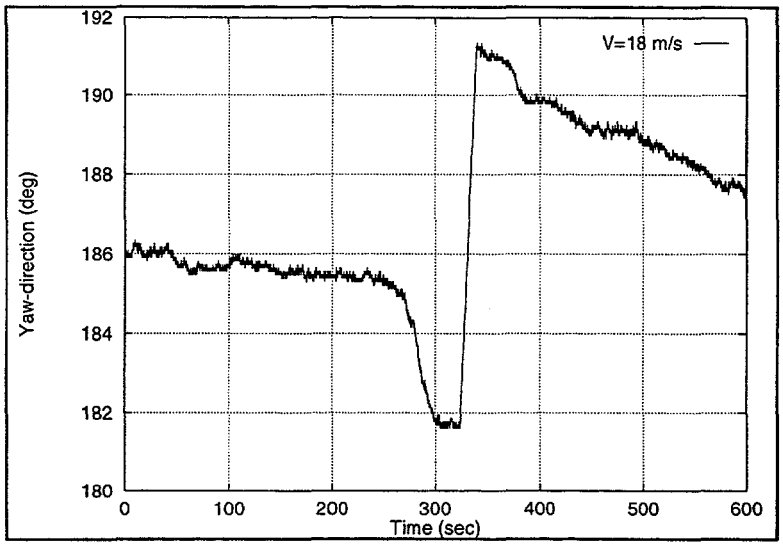

Figure 3.3-26 Time-track of measured yaw direction at 18 m/s.

4. Conclusion

Comparison of measurements and predictions shows that the model is good compared to state of the art in aeroelastic wind turbine modelling. The ability of the model to predict importance of large yaw misalignment has not been tested. The turbulence model used for the validation is the Mann model (Mann, 1994).

One limitation of the model is that at normal operation it underestimates the fatigue loads in stall, i.e. at mean wind speeds above 15 m/s. The underestimation is not important for the investigation of parameter sensitivity of turbine loads, which is the aim of the modelling, but if using the model for other purposes this might be important.

5. References

- Aagaard Madsen, H. (1991). Aerodynamics of a Horizontal-Axis Wind Turbine in Natural Conditions. Risø-M-2903. Risø National Laboratory, Roskilde, Denmark.

- Abbot, I.H. and Doenhoff, A.E. (1959). Theory of Wing Sections. Dover Publications Inc, New York, USA.

- Mann, J. (1994). Models in Micrometeorology. Risø-R-727(EN). Risø National Laboratory, Roskilde, Denmark.

- Petersen, S.M (1994). Wind Turbine Test. NORDTANK NTK 500/37. System Test. Risø-R-714 (EN). Risø National Laboratory, Roskilde, Denmark.

- Rasmussen, F. et al (1988). Investigations of Aerodynamics, Structural Dynamics and Fatigue on Danwin 180 kW. Risø-M-2727. Risø National Laboratory, Roskilde, Denmark.

- Thirstrup Petersen, J. (1990). Kinematically Nonlinear Finite Element Model of a Horizontal Axis Wind Turbine. Part 1 and 2. Risø National Laboratory, Roskilde, Denmark.

- Vølund, P. and Petersen, S.M. (1996). Predictions of Loads on Wind Turbines in a Complex Terrain. Risø-I-1038 (EN). Risø National Laboratory, Roskilde, Denmark.

- Øye, Stig (1991). Dynamic Stall Simulated as Time Lag of Separation. Dept. of Fluid Mechanics, Technical University of Denmark.

6. Appendix Choice of stall model parameter

The choice of time-lag parameter (k in the expression for the model time constant: $\tau=k*C/V$) for the Stig Øye stall model (Øye, 1991) was of special concern in this project, because comparison with measurements at 18 m/s proved a high sensitivity to the parameter of the aeroelastic code, HawC. On the background of the PSD's shown in the following pages a value of 12 was chosen for the simulations presented in this report.

The predicted results are found to compare very well with measurements, but the value of 12 is very high in comparison with values known to be used with good results for other codes, and this is a warning that the code of HawC should be examined again to investigate the cause of the difference.

Figure 6-1 shows the tilt moment at 18 m/s for a measurement at predictions with k equal to 4, 8 and 12. 12 is obviously giving the result closest to the measurements. The corresponding shaft bending moment in Figure 6-2 confirms this fact, and so does the PSD's of shaft torque, flapwise blade moment and edgewise blade moment in Figure 6-3, Figure 6-4 and Figure 6-5. In the following pages PSD's of the same 5 signals at 14 and 10 m/s are shown. At 14 m/s there is a slight indication that 12 is the best choice, whereas at 10 m/s no clear difference is seen between choosing 4, 8 or 12.

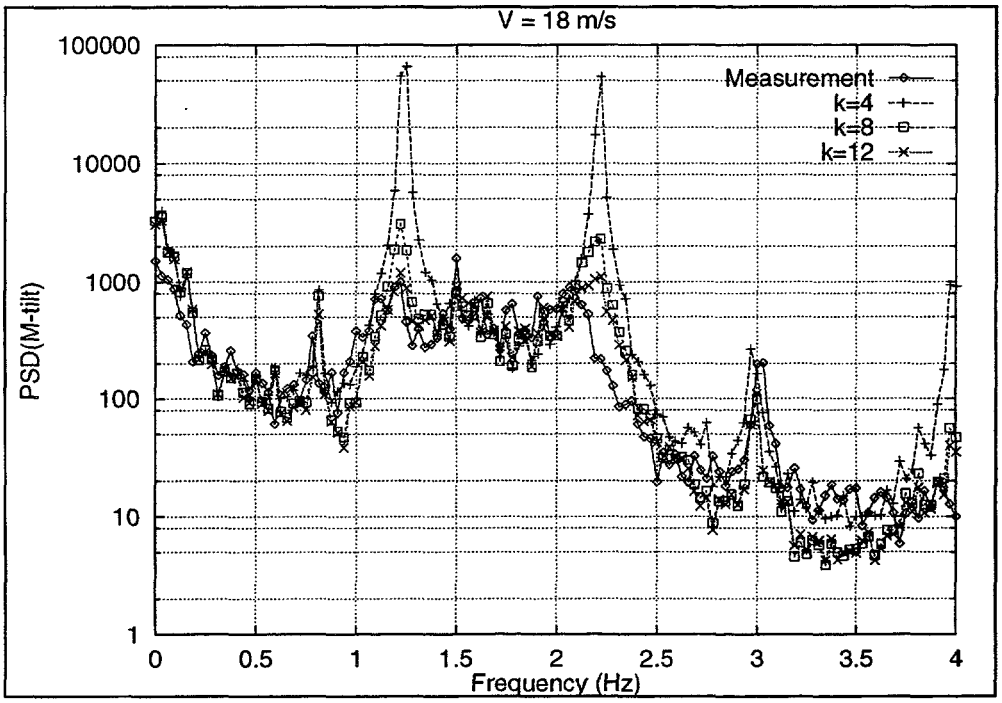

Figure 6-1 Tilt moment. V=18 m/s .

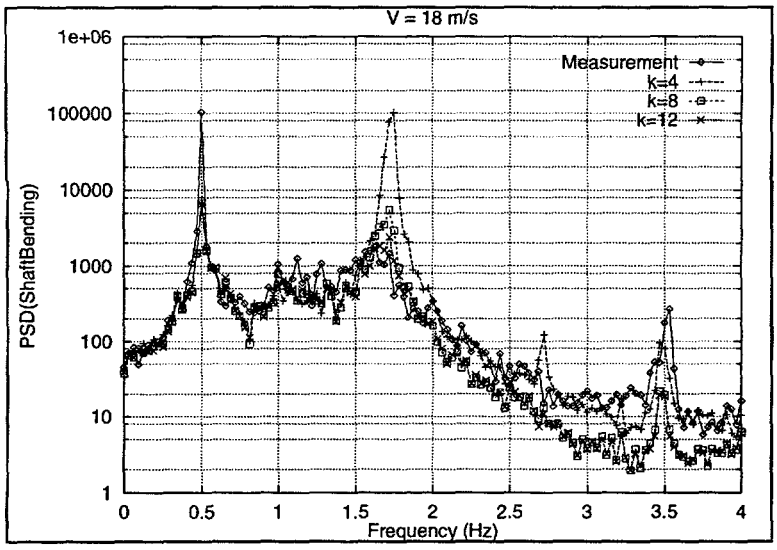

Figure 6-2 Shaft Bending Moment. V=18 m/s.

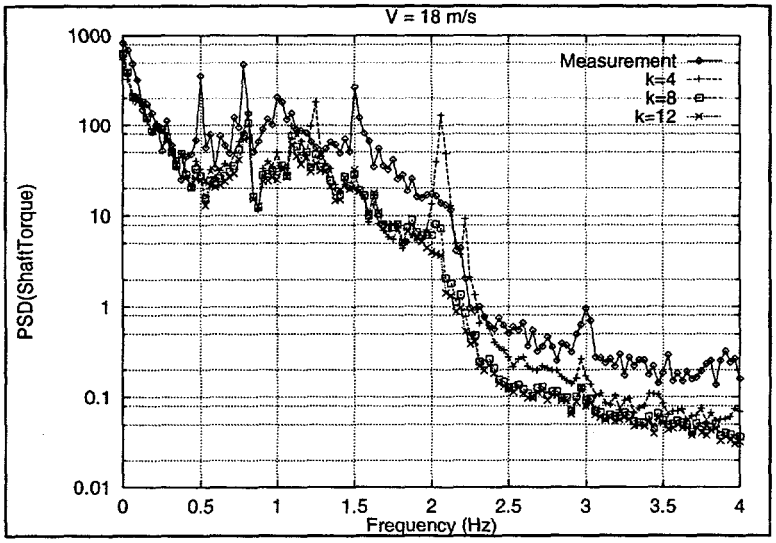

Figure 6-3 Shaft Torque. V=18 m/s.

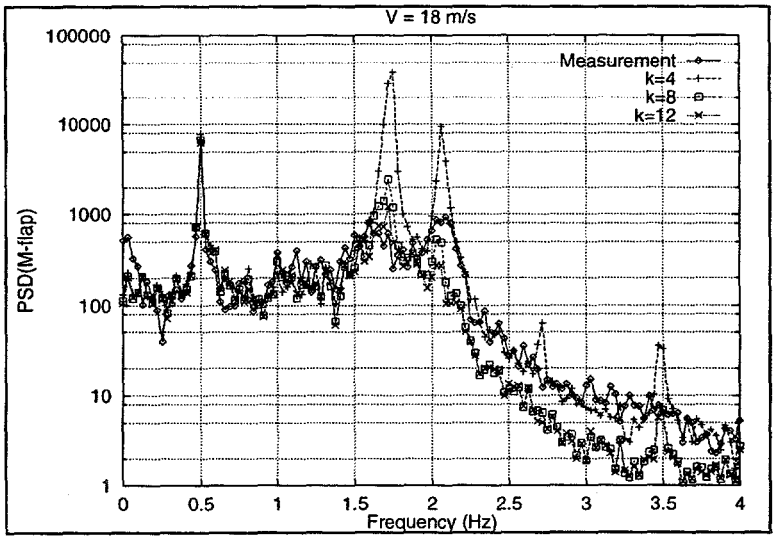

Figure 6-4 Flapwise blade root bending moment. V=18 m/s.

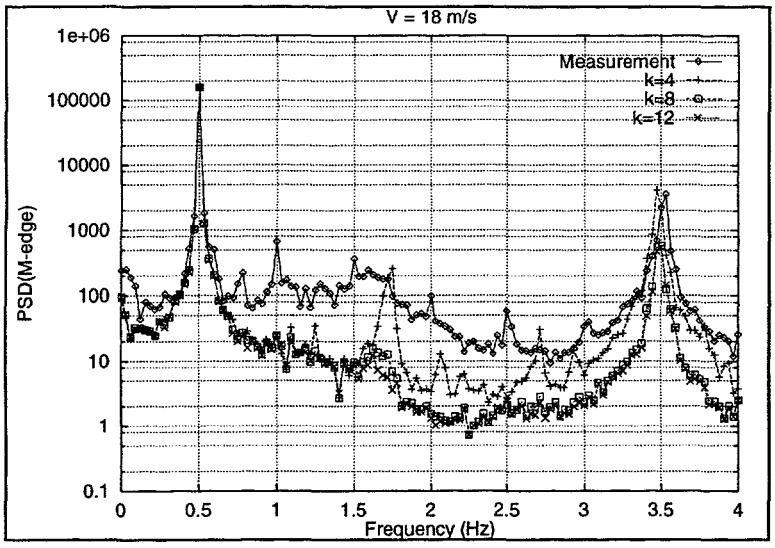

Figure 6-5 Edgewise blade root bending moment. V=18 m/s.

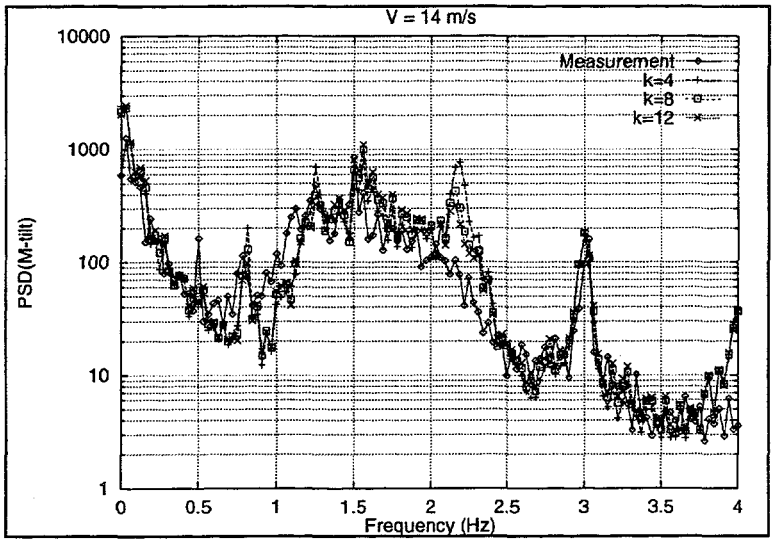

Figure 6-6 Tilt moment. V=14 m/s .

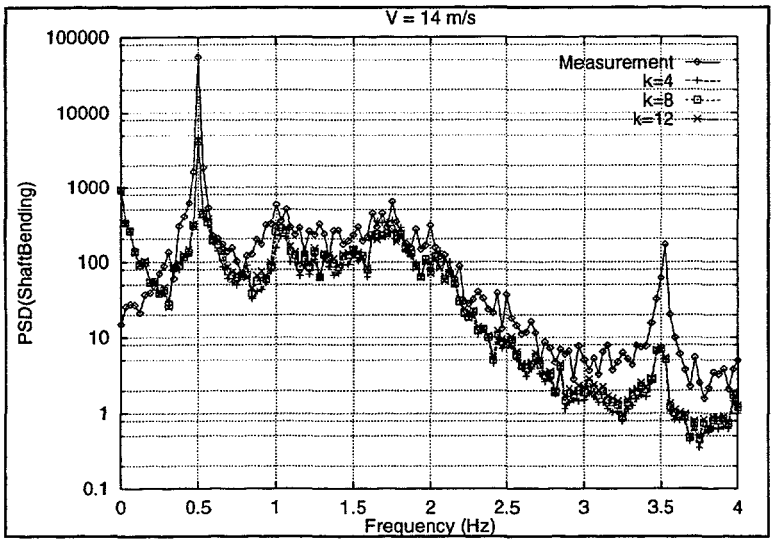

Figure 6-7 Shaft Bending Moment. V=14 m/s.

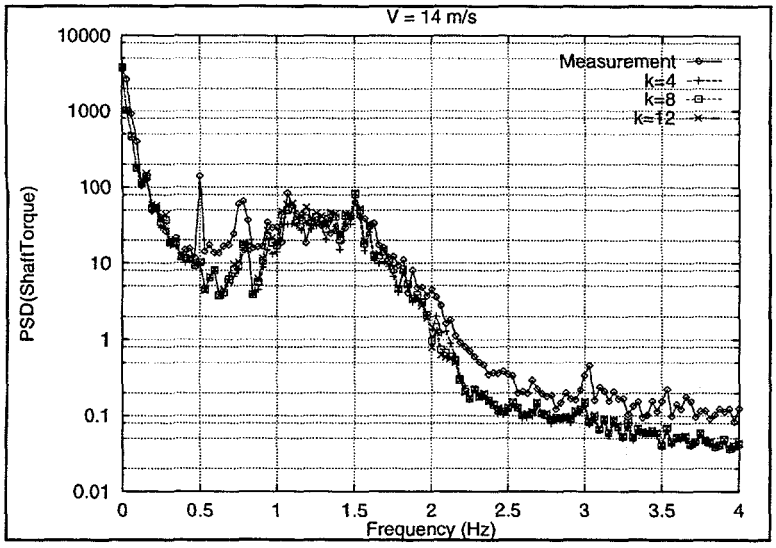

Figure 6-8 Shaft Torque. V=14 m/s.

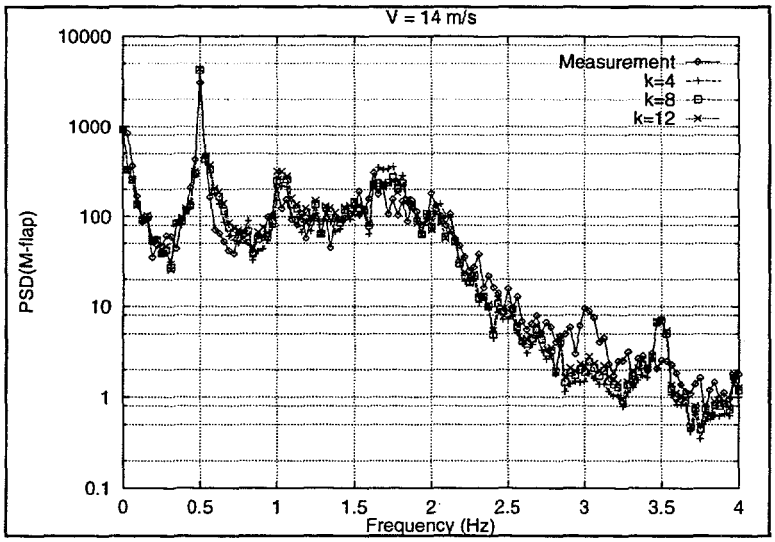

Figure 6-9 Flapwise blade root bending moment. V=14 m/s.

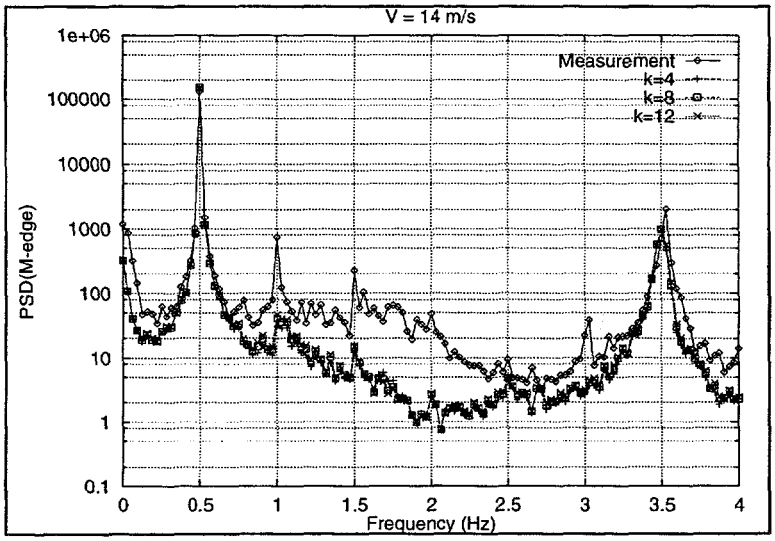

Figure 6-10 Edgewise blade root bending moment. V=14 m/s.

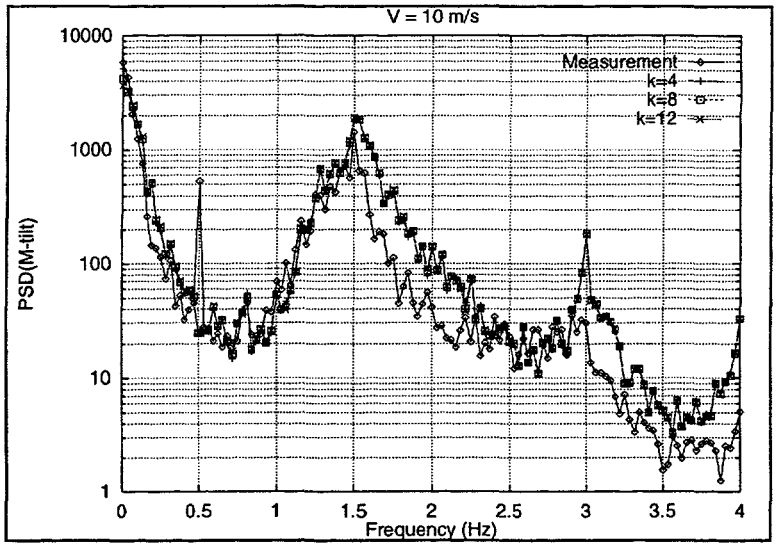

Figure 6-11 Tilt moment. V=10 m/s.

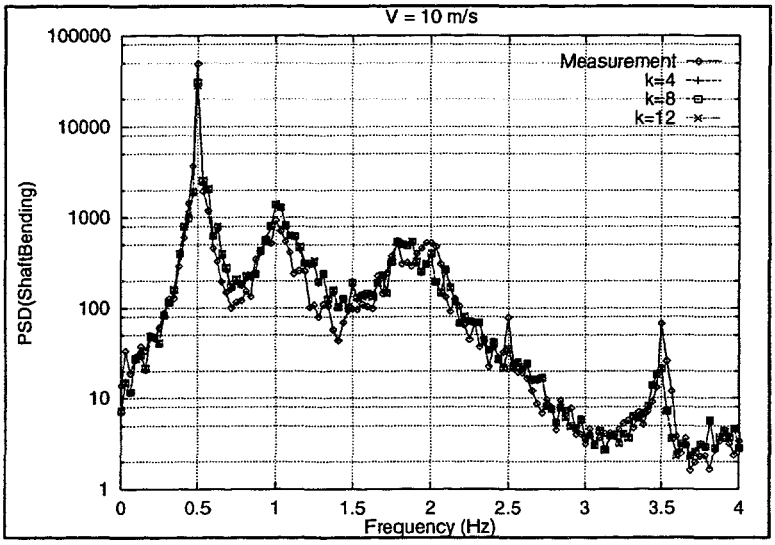

Figure 6-12 Shaft Bending Moment. V=10 m/s.

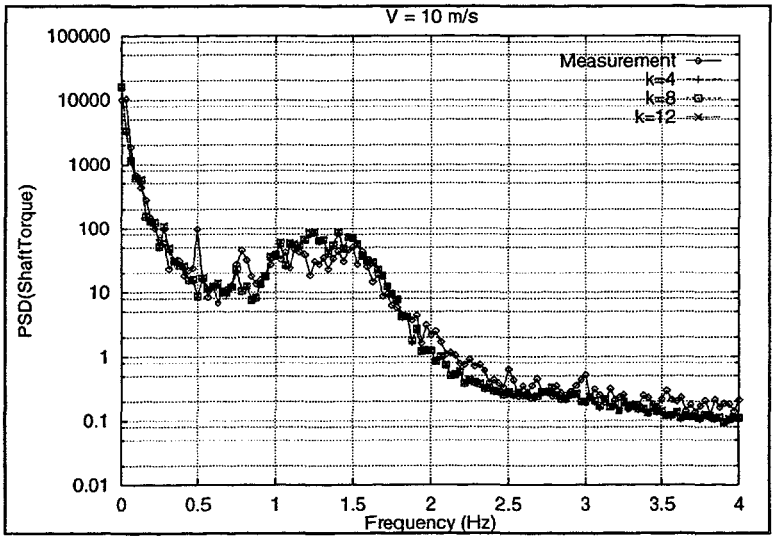

Figure 6-13 Shaft Torque. V=10 m/s.

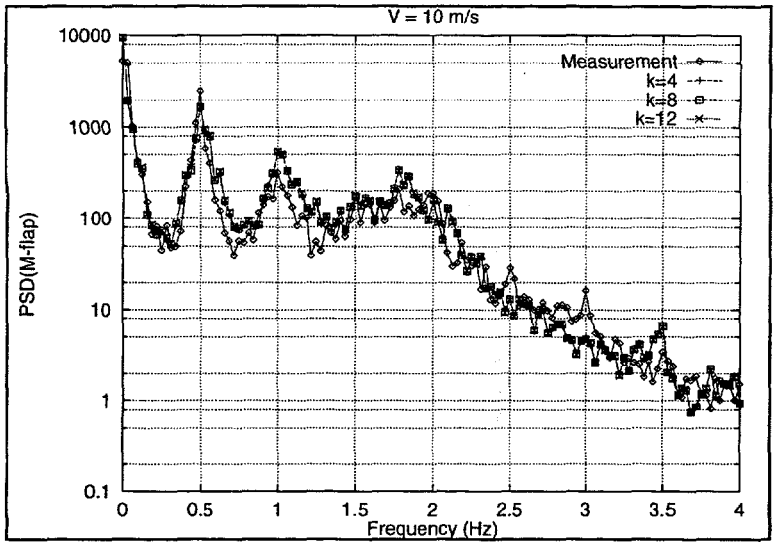

Figure 6-14 Flapwise blade root bending moment. V=10 m/s.

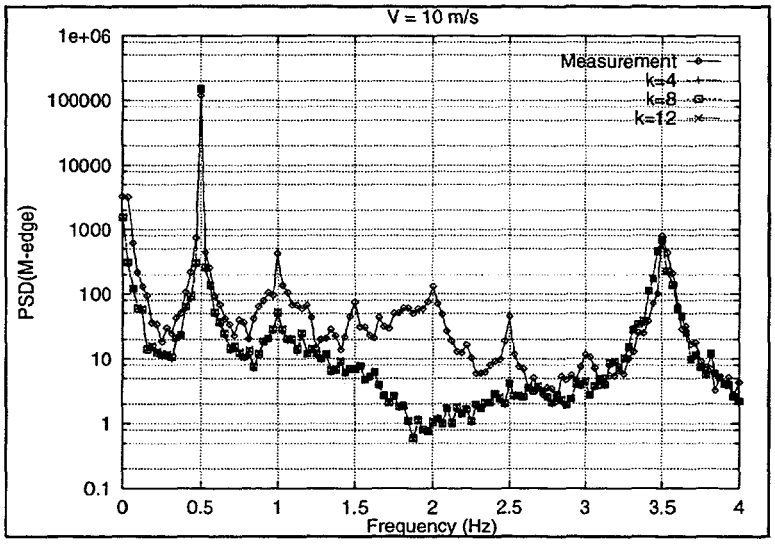

Figure 6-15 Edgewise blade root bending moment. V=10 m/s.

Bibliographic Data Sheet **Risø-R-1006(EN)**

Title and authors

Validation of aeroelastic model of Nordtank 500/37

Per Vølund and Søren Markkilde Petersen

ISBN 87-550-2349-5

ISSN 0106-2840

Department or group
Wind Energy and Atmospheric Physics Department

Date
November 1997

Groups own reg. number(s)
VIM-3744-00

Project/contract No(s)
JOR3-CT95-0033

Pages	Tables	Illustrations	References
32	1	49	8

Abstract (max. 2000 characters)

An aeroelastic model of the stall controlled wind turbine Nordtank 500/37 is validated by comparison of predictions and measurements. The aeroelastic code used is HawC, which has been developed at Risø, and the turbulence model is the Mann model. The measurements used for validation were carried out in the flat terrain of Risø. The model was developed for investigation of load sensitivity to wind and turbulence parameters for complex terrain in the project COMTERID.

The model is found to be good compared to state of the art aeroelastic wind turbine modelling, but the ability of the model to predict the importance of large yaw misalignment is not tested. One limitation of the model is an underestimation of fatigue loads in stall, but for the investigation of parameter sensitivity of complex terrain induced loads, which is meant to be the primary use of the model, this is not important.

Descriptors INIS/EDB

AERODYNAMICS; COMPUTERIZED SIMULATION; ELASTICITY; EXPERIMENTAL DATA; HORIZONTAL AXIS TURBINES; TURBULENCE; WIND LOADS.

Available on request from Information Service Department, Risø National Laboratory,
(Afdelingen for Informationsservice, Forskningscenter Risø), P.O.Box 49, DK-4000 Roskilde, Denmark.
Telephone +45 46 77 40 04, Telefax +45 46 77 40 13